Origin of the long-wavelength magnetic modulation in $Ca_3Co_2O_6$

L. C. Chapon*
ISIS Facility, Rutherford Appleton Laboratory–STFC, Chilton, Didcot, OX11 0QX, United Kingdom
(Received 20 November 2008; published 23 November 2009)

The origin of the long-wavelength incommensurate magnetic structure of $Ca_3Co_2O_6$ is discussed considering possible interchains super-superexchange paths. The experimental value of the propagation vector $k=(0,0,\Delta)$ with $\Delta>1$ can be reproduced only if one considers the next-nearest super-superexchange interaction. A spin-dimer analysis using the extended Huckel tight-binding method confirms that, despite longer interatomic Co-Co distances, the latter interaction is indeed much stronger. The stability of the observed structure with respect to certain commensurate states is discussed.

DOI: 10.1103/PhysRevB.80.172405 PACS number(s): 75.50.Ee, 75.30.Gw, 75.30.Fv

The magnetic properties of $Ca_3Co_2O_6$ have attracted considerable interest in the last decade, as this compound is considered as an exact experimental realization of an Ising triangular lattice.[1] Among the properties long debated were the nature of the ordered magnetic state and the still ambiguous origin of the steps in the magnetization measurements at low temperature,[2–4] reminiscent of that seen in single-molecule magnets.[5]

In the $Ca_3Co_2O_6$ crystal structure only one of the two inequivalent Co^{3+} sites, in trigonal prismatic coordination, is magnetic with a spin-state $S=2$ and a large orbital contribution. It is well established that these magnetic sites are strongly coupled ferromagnetically within chains running along the c axis and that adjacent chains on the triangular lattice are coupled by weak antiferromagnetic (AFM) interactions in the ab plane.[6] Major insight into the physics of these systems have been given by density-functional theory studies.[7,8] However, the magnetic properties to date have been undertaken mostly in the framework of a quasi-two-dimensional (2D) lattice, i.e., considering a simple ferromagnetic stacking of AFM triangular planes neglecting the true three-dimensional nature of the exchange interactions. Such approximation, justified in the light of the magnetic structures reported earlier,[6] has been challenged by the recent work of Agrestini *et al.*[9,10] Using first magnetic x-ray diffraction[9] and then neutron diffraction,[10] these authors have unambiguously established that the magnetic structure is in fact incommensurate, with a modulation along the c axis of very long periodicity ($\sim$1000 Å). Clearly, such a structure cannot be stabilized in the quasi-2D limit since the only magnetic interaction along c is ferromagnetic. In order to understand the origin of the proposed ground state it is important to reconsider all possible exchange interactions in the system.

In the present communication, I analyze the energy of the magnetic structure considering only isotropic exchange terms and two different super-superexchange (SSE) interactions forming helical paths between adjacent chains of the triangular lattice. In this framework, the observed magnetic modulation cannot be explained by considering only the nearest neighbor (noted J_2) AFM SSE but requires the presence of a nonvanishing next-nearest AFM SSE terms (J_3) which can uniquely stabilize the experimental value of the magnetic propagation vector. A spin-dimer analysis using the extended Hukel tight-binding (EHTB) method, shows that J_3 is indeed the predominant interchain coupling term due to a stronger overlap in the molecular orbital involving the Co 3d xz and yz state. While the observed structure corresponds to the first-ordered state, for small values of J_3 its exchange energy is energetically unfavorable with respect to certain commensurate structures with equal moments, suggesting that the former is stabilized due to a lower entropy.

The magnetic structure reported by Agrestini *et al.*[10] corresponds to a longitudinal amplitude modulation propagating along the c axis of the hexagonal cell (space group $R\bar{3}m$, hexagonal setting),[11] as illustrated in Fig. 1. In agreement with previous reports, the magnetic moments are aligned along the c axis, fixed by the strong single-ion axial anisotropy.[3,4] However, what differs from previous studies is the amplitude modulation or spin-density wave (SDW), i.e., the existence of regions in *each chain* with quasinull ordered moments. It implies that the magnetic configuration within a triangular unit (three adjacent chains) approaches C1=(+,−,0) *only* at some particular point along the chain (see Fig. 1), unlike the proposed partially disordered antiferromagnet (PDA) structure[12,13] which maintains this configuration along the entire chain. At other lattice points the configuration is almost C2=$(+\frac{1}{2},+\frac{1}{2},-\frac{1}{2})$ (Fig. 1) and, if the structure is truly incommensurate, any other intermediate situations between C1 and C2 are found somewhere in the crystal. Such mag-

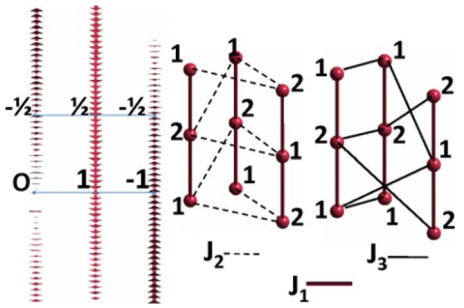

FIG. 1. (Color online) Left: Sketch of the experimental magnetic structure of $Ca_3Co_2O_6$ showing the longitudinal amplitude modulation for three adjacent chains running along the c axis (25 unit cells are displayed). Specific values of the in-plane magnetic configuration $(0,1,-1)$ and $(-\frac{1}{2},\frac{1}{2},-\frac{1}{2})$ are also shown. Middle and right: Schematic drawing of interchain super-superexchange paths between cobalt site 1 (1) and site 2 (2) for J_2 (middle) and J_3 (right). The ferromagnetic intrachain coupling (J_1) is also shown.

netic arrangement usually originates from competing interactions along the chains in the presence of axial anisotropy since, for isotropic systems, competing interactions would simply lead a noncollinear state with fully ordered moments. The propagation vector in the hexagonal setting is $\mathbf{k}_H = 2\pi(0,0,\Delta)$, with $\Delta \sim 1.01$ at 18 K. Δ varies with temperature, suggesting a true incommensurability rather than a locking at a particular fractional value. The fact that $\Delta > 1$ is of particular importance, as will be discussed in the following sections.

For describing the magnetic structure, it is actually more convenient to work in the primitive rhombohedral setting,[11] which will be used in the rest of the communication. In the rhombohedral setting of space group $R\bar{3}m$, the unit-cell dimensions are $a=b=c=6.274$ Å and $\alpha=\beta=\gamma=92.53°$. There are two magnetic Co sites per unit cell, S_1 and S_2, at respective fractional coordinates $(\frac{1}{4},\frac{1}{4},\frac{1}{4})$ and $(\frac{3}{4},\frac{3}{4},\frac{3}{4})$. In this setting, the co-chains are running along the [1,1,1] direction (also the direction of axial anisotropy), and the propagation vector is $\mathbf{k}=2\pi(\frac{\Delta}{3},\frac{\Delta}{3},\frac{\Delta}{3})$. The magnetic structure derived experimentally by Agrestini *et al.*[10] corresponds to a mode belonging to a single irreducible representation, in agreement with the theory of second-order transition, noted Γ_1 in Kovalev's notation.[14] For this mode, the cobalt magnetic moments $\mathbf{M}$ on S_1 ($\mathbf{M}_1$) and S_2 ($\mathbf{M}_2$), in a unit-cell translated by $\mathbf{R}_L=(R_x,R_y,R_z)$ with respect to the zeroth-cell, are written as follows:

$$\mathbf{M}_1(\mathbf{R}_L) = \mathbf{M}\cos(\mathbf{k}\cdot\mathbf{R}_L),$$

$$\mathbf{M}_2(\mathbf{R}_L) = -\mathbf{M}\cos(\mathbf{k}\cdot\mathbf{R}_L + \pi\Delta), \tag{1}$$

where $\mathbf{M}$ is a vector pointing along [1,1,1], whose length is the amplitude of the SDW. The energy of this structure can be calculated, in the limit of isotropic exchange interactions, considering the intrachain ferromagnetic interaction J_1, interchain SSE interactions and a phenomenological single-ion anisotropy term DS^2. Given the crystallographic parameters, two SSE interactions, mediated through Co-O-O-Co paths, must be taken into account. They correspond to interchain nearest (J_2) and next-nearest (J_3) neighbors, at interatomic Co-Co distances of 5.513 Å and 6.274 Å respectively. Each site (S_1 or S_2) has six neighbors connected through J_2 and six neighbors connected through J_3. The list of neighbors is given in Table I. These SSE interactions, form helical paths between Co sites of adjacent chains within a triangular motif, as shown in Fig. 1, clearly competing with the ferromagnetic intrachain exchange, when J_2 or/and J_3 are antiferromagnetic. The energy of the magnetic mode found experimentally is easily calculated by summing on all lattice cells ($\mathbf{R}_L$). The total energy, taking the convention $J<0$ for AFM interactions, is decomposed into a normal (E_N) and umklapp (E_U) terms,

$$E_N = \frac{1}{2}M^2\left[J_1\cos(\pi\Delta) + 3J_2\cos\left(\frac{\pi\Delta}{3}\right) - 3J_3\cos\left(\frac{2\pi\Delta}{3}\right) + D\right], \tag{2}$$

TABLE I. List of super-superexchange paths for $Ca_3Co_2O_6$. S_1 and S_2 refer to the two Co positions in the primitive rhombohedral unit-cell, at fractional coordinate of $(\frac{1}{4},\frac{1}{4},\frac{1}{4})$ and $(\frac{3}{4},\frac{3}{4},\frac{3}{4})$ respectively, while R_m refer to the translation of site j with respect to site i.

SSE interaction	Site i	Site j	R_m
J_2	S_1	S_2	(−1,0,0)
	S_1	S_2	(0,−1,0)
	S_1	S_2	(0,0,−1)
	S_1	S_2	(−1,−1,0)
	S_1	S_2	(−1,0,−1)
	S_1	S_2	(0,−1,−1)
J_3	$S_{1(2)}$	$S_{1(2)}$	(1,0,0)
	$S_{1(2)}$	$S_{1(2)}$	(−1,0,0)
	$S_{1(2)}$	$S_{1(2)}$	(0,1,0)
	$S_{1(2)}$	$S_{1(2)}$	(0,−1,0)
	$S_{1(2)}$	$S_{1(2)}$	(0,0,1)
	$S_{1(2)}$	$S_{1(2)}$	(0,0,−1)

$$E_U = \frac{M^2}{2N}\sum_{R_l} J_1[\cos(2\mathbf{k}\cdot\mathbf{R}_L)\cos(\pi\Delta)] + 3J_2\left[\cos(2\mathbf{k}\cdot\mathbf{R}_L)\cos\left(\frac{\pi\Delta}{3}\right)\right] - 3J_3\left[\cos(2\mathbf{k}\cdot\mathbf{R}_L)\cos\left(\frac{2\pi\Delta}{3}\right)\right] + D[\cos(2\mathbf{k}\cdot\mathbf{R}_L)]. \tag{3}$$

When the structure is incommensurate, as found experimentally, one needs to consider only the nonvanishing normal term in Eq. (2). By derivating E_N with respect to Δ, we obtain

$$J_1\sin(\pi\Delta) + J_2\sin\left(\frac{\pi\Delta}{3}\right) - 2J_3\sin\left(\frac{2\pi\Delta}{3}\right) = 0. \tag{4}$$

The parameter Δ varies in the first Brillouin zone, i.e., $\Delta \leq 3/2$. Let's consider FM J_1 (>0) and AFM J_2 and J_3. By imposing nearest interchain neighbors only ($J_2<0$, $J_3=0$), there are solutions uniquely for $\Delta \leq 1$, since the terms in J_1 and J_2 must have opposite signs in Eq. (4). However, if one considers only FM J_1 and $J_3<0$, it is possible to stabilize solutions with $\Delta > 1$, as observed experimentally. In particular, reproducing the experimental value of $\Delta \sim = 1.01$ requires $J_3 = -0.018J_1$.

Fresard *et al.*[15] already singled-out that J_3 is a relevant parameter, based on a shorter O-O distance than that of J_2. This argument is often valid, as shown by the work of Whangbo and co-workers in a variety of insulating oxides.[16] Based on the crystal structure derived by neutron diffraction at 18 K, the O-O distance of 2.908 Å for J_3 is indeed shorter than for J_2 (2.937 Å), despite a much longer Co-Co distance (6.274 Å instead of 5.513 Å). The dihedral angles along the J_3 Co-O-O-Co path also maximize the orbital overlap as shown next. The SSE energy can be derived semiquantita-

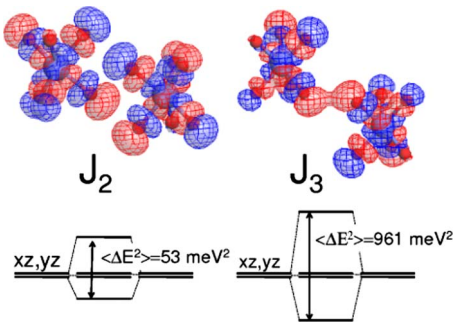

FIG. 2. (Color online) Bounding molecular orbitals (involving the Co d_{xz}, d_{yz} levels) of the dimer $Co_2O_{12}^{18-}$ corresponding to super-superexchange paths along J_2 and J_3, calculated from the extended Huckel tight-binding method. The energy diagram shows the corresponding values of the squared energy difference between bounding and antibounding states (see text for details).

tively by a spin-dimer analysis based on the extended Huckel tight-binding method using double-ξ Slater orbitals for the O s and p states and Co d states.[16] Here, each dimer $Co_2O_{12}^{18-}$ along J_2 and J_3 is considered in turn and the exchange energy is directly estimated from the square of the energy difference between the bounding and antibounding levels.[16] In the present case, one needs to take into account the multielectron configuration (d^4, $S=2$ ground state). Since the point symmetry is high ($\bar{3}m$), only the overlap between nonorthogonal orbitals is relevant for the calculations as explained in.[16] The spin-dimer analysis has been performed with the program CAESAR 2.0,[17] using slater parametrizations for Co and O atoms given in.[18] In trigonal prismatic configuration (point group $\bar{3}m$), the Co d orbitals are splitted into one singly degenerate level (z^2) and two doubly degenerate levels: (x^2-y^2, xy) and (xz,yz). The z^2 level is fully occupied and does not contribute. The four unpaired electrons occupy the doubly-degenerated levels, the latter lying higher in energy. The spin-dimer analysis shows that the energy difference between bounding and antibounding states involving the (x^2-y^2, xy) orbitals are not dramatically different for J_2 and J_3 (considered alone they would lead to $J_2=1.6J_3$). The dimer levels involving the Co (xz,yz) states, form two nonbounding molecular orbitals (no interaction within the numerical accuracy) and a pair of bounding and antibounding state, both in the cases of the J_2 and J_3 dimers, as displayed in Fig. 2. However the energy gap separating the two latter states is much stronger in the case of J_3 (31 meV) than for J_2 (7.3 meV), providing a coupling through these orbitals about 20 times stronger for J_3. This result, even though semiquantitative, supports entirely the conclusions conveyed previously in the analysis of the exchange energy, and the initial assumption of Fresard *et al.*[15] highlighting the crucial role of the next-nearest SSE interaction in this system.

I now turn to the stability of the SDW structure. One can easily shows that it corresponds to the first ordered state, which can be derived as a function of the propagation vector $k=(x,y,z)$ for various sets of exchange integrals $\{J_{ij}\}$. Here the anisotropy, whose effect is to stabilize a SDW rather than a noncollinear configuration but does not affect the propagation, is not considered. The ground state is obtained by calculating the eigenvector corresponding to the maximum eigenvalues of the Fourier transform of the exchange-integral matrix ξ_{ij},[19]

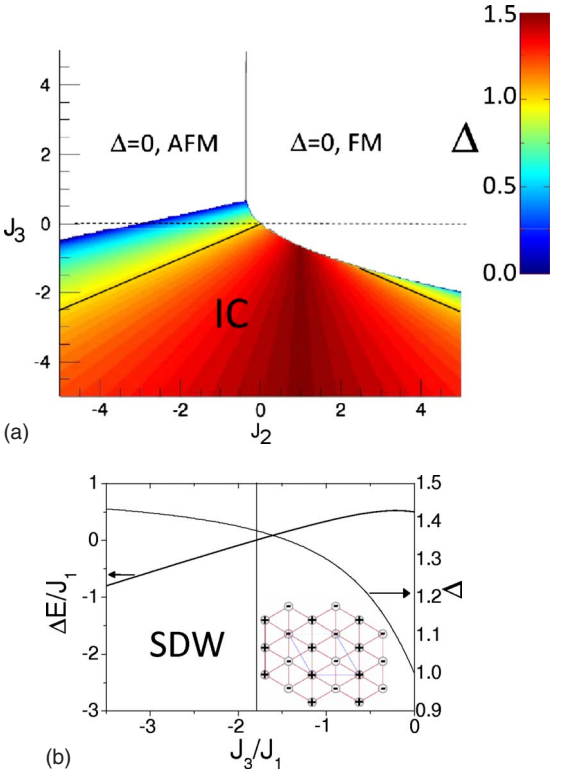

FIG. 3. (Color online) (a) First ordered state of $Ca_3Co_2O_6$ for isotropic exchange interactions, considering a unitary ferromagnetic intrachain coupling ($J_1=1$) and a wide range of super-superexchange interchain coupling parameters (J_2,J_3). The value of propagation vector component Δ is color coded. (b) Energy difference between a SDW and the commensurate structure with $k=(\frac{1}{2},\frac{1}{2},0)$ shown in the inset as a function of J_3/J_1 or Δ.

$$\xi_{ij}(\mathbf{k},\{J_{ij}\}) = \sum_m J_{ij}(\mathbf{R}_m)\exp(-i\mathbf{k}\cdot\mathbf{R}_m). \tag{5}$$

The indices i and j refer to the magnetic atoms in a primitive cell (S_1 and S_2). $J_{ij}(R_m)$ is the isotropic exchange interaction between the spins of atoms i and j in units cells separated by the lattice vector R_m, as listed in Table I. In our case, there are only two magnetic atoms per unit-cell and the two by two Hermitian ξ_{ij} matrix is simply written:

$$\xi_{ij}(\mathbf{k},\{J_{ij}\}) = \begin{pmatrix} A & B \\ B^* & A \end{pmatrix}, \tag{6}$$

where:

$$A = 2J_3[\cos(x)+\cos(y)+\cos(z)]$$

$$B = J_1(1+e^{i(x+y+z)}) + J_2(e^{ix}+e^{iy}+e^{iz}+e^{i(x+y)}+e^{i(x+z)} + e^{i(y+z)}).$$

The phase diagram was generated numerically with the program ENERMAG,[20] performing a grid search of $\mathbf{k}$ within the first Brillouin zone for various sets of exchange parameters.

J_1 was fixed to 1, while J_2 and J_3 were varied between −5 and +5. As expected from the form of ξ_{ij}, invariant by permutation of x, y, and z, the only type of propagation vector stabilized varies along a line with $x=y=z$. The phase diagram is represented in Fig. 3. In two large regions, the propagation vector $\mathbf{k}=0$ is stabilized, with either FM or AFM configurations. In addition, there is a large region of incommensurability corresponding to $\mathbf{k}=2\pi(\frac{\Delta}{3},\frac{\Delta}{3},\frac{\Delta}{3})$. As already derived from analysis of the Γ_1 magnetic mode energy, the line $J_3=0$ stabilizes only $\Delta\leq 1$ and the experimental value of $\Delta=1.01$ requires $J_3\neq 0$. However, one can also show that an ordered commensurate (CM) phase with equal moments, not obtained as first ordered state, has a lower exchange energy than the SDW structure. The structure, presented in the inset of Fig. 3 propagates with a single $\mathbf{k}=(\frac{1}{2},\frac{1}{2},0)$. Every magnetic site is fully ordered and has four out of its six first neighbors aligned antiparallel and two aligned parallel. For values of $|J_3/J_1|<1.7$, the exchange energy of this structure is lower than the SDW, as presented in Fig. 3. Moreover, the values of Δ decrease on cooling according to the resonant x-ray study,[9] i.e., the CM structure should be increasingly favorable. This indicates that the SDW structure, as observed, is stabilized only thanks to a smaller configuration entropy. The presence of competing terms in the free energy (exchange and entropy) could explain the crossover regime observed at the so-called freezing temperature $T\sim 18$ K, temperature below which the coherence length of the SDW is suddenly reduced.[10]

In conclusion, I have shown that the long-wavelength magnetic modulation in $Ca_3Co_2O_6$ originates from the existence of interchain AFM super-superexchange terms forming helical paths running between adjacent chains of the triangular motif. The analysis of the energy and first ordered ground state in the isotropic exchange limit, and a spin-dimer analysis, points to the next-nearest-exchange interaction as the critical parameter to reproduce the propagation found experimentally. It is argued that this phase it stabilized thanks to a lower configuration entropy than other configurations with constant moments.

I would like to acknowledge Daniel Khomskii and Paolo G. Radaelli for fruitful discussions and critical reading of the manuscript.

*l.c.chapon@rl.ac.uk

[1] G. H. Wannier, Phys. Rev. **79**, 357 (1950).
[2] H. Kageyama, K. Yoshimura, K. Kosuge, M. Azuma, M. Takano, H. Mitamura, and T. Goto, J. Phys. Soc. Jpn. **66**, 3996 (1997).
[3] H. Kageyama, K. Yoshimura, K. Kosuge, H. Mitamura, and T. Goto, J. Phys. Soc. Jpn. **66**, 1607 (1997).
[4] A. Maignan, C. Michel, A. C. Masset, C. Martin, and B. Raveau, Eur. Phys. J. B **15**, 657 (2000).
[5] A. Maignan, V. Hardy, S. Hébert, M. Drillon, M. R. Lees, O. Petrenko, D. M. K. Paul, and D. Khomskii, J. Mater. Chem. **14**, 1231 (2004).
[6] S. Aasland, H. Fjellvag, and B. Hauback, Solid State Commun. **101**, 187 (1997).
[7] V. Eyert, C. Laschinger, T. Kopp, and R. Fresard, Chem. Phys. Lett. **385**, 249 (2004).
[8] H. Wu, M. W. Haverkort, Z. Hu, D. I. Khomskii, and L. H. Tjeng, Phys. Rev. Lett. **95**, 186401 (2005).
[9] S. Agrestini, C. Mazzoli, A. Bombardi, and M. R. Lees, Phys. Rev. B **77**, 140403(R) (2008).
[10] S. Agrestini, L. C. Chapon, A. Daoud-Aladine, J. Schefer, A. Gukasov, C. Mazzoli, M. R. Lees, and O. A. Petrenko, Phys. Rev. Lett. **101**, 097207 (2008).
[11] *International Tables for Crystallography, Volume A*, edited by Th. Hahn (Springer-Verlag, 2006).
[12] M. Mekata, J. Phys. Soc. Jpn. **42**, 76 (1977).
[13] K. Wada and T. Ishikawa, J. Phys. Soc. Jpn. **52**, 1774 (1983).
[14] O. V. Kovalev, *Irreducible Representations of Space Groups* (Gordon and Breach, New York, 1965).
[15] R. Fresard, C. Laschinger, T. Kopp, and V. Eyert, Phys. Rev. B **69**, 140405(R) (2004).
[16] M.-H. Whangbo, D. Dai, and H. J. Koo, Solid State Sci. **7**, 827 (2005).
[17] J. Ren and M.-H. Whangbo, *CAESAR 2.0 Primecolor Software, Inc.*, Madison, WI, 1998.
[18] H.-J. Koo, K.-S. Lee, and M.-H. Whangbo, Inorg. Chem. **45**, 10743 (2006).
[19] M. J. Freiser, Phys. Rev. **123**, 2003 (1961).
[20] G. Rousse, J. Rodriguez-Carvajal, C. Wurm, and C. Masquelier, Solid State Sci. **4**, 973 (2002).